JOC The Journal of Organic Chemistry

Article

pubs.acs.org/joc

Mutual Interference between Intramolecular Proton Transfer Sites through the Adjoining π-Conjugated System in Schiff Bases of Double-Headed, Fused Salicylaldehydes

Hirohiko Houjou,* Hajime Shingai, Keisuke Yagi, Isao Yoshikawa, and Koji Araki

Institute of Industrial Science, The University of Tokyo, 4-6-1 Komaba, Meguro-ku, Tokyo 153-8505, Japan

Supporting Information

ABSTRACT: We synthesized two constitutionally isomeric bis(iminomethyl)-2,6-dihydroxynaphthalenes, namely, α,α-diimines **1** and β,β-diimines **2**, which can be formally represented as fused salicylaldimines with resonance-assisted hydrogen-bonding sites. Spectroscopic data show that the OH/OH, NH/OH, and NH/NH forms of **1** were in equilibrium in solution and that the proportion of the NH-bearing tautomers increased as the solvent polarity increased. The UV spectra of thin solid films of **1** with various types of hydrogen-bonding networks differed from one another, and the spectral profiles were markedly temperature dependent, whereas the spectra of **1** in the molten state showed quite similar profiles. In contrast, **2** existed predominantly as the OH/OH form irrespective of the solvent polarity or crystal packing. Quantum chemical calculations suggest that the difference between the probabilities of intramolecular proton transfer in **1** and **2** can be explained in terms of the interplay between the resonance-assisted hydrogen-bonding sites and the adjoining π-conjugated system.

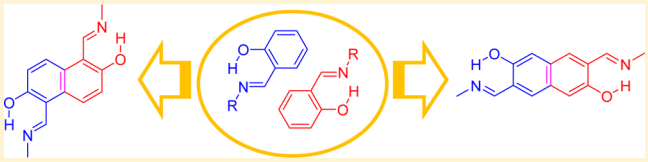

INTRODUCTION

Salicylaldehyde Schiff bases have attracted interest for a long time, owing to photochromic and thermochromic phenomena that accompany intramolecular proton transfer (PT) in these molecules.[1,2] The potential energy surface, which includes the phenol-imine (OH form) and keto-enamine (NH form) tautomers, determines the probability of intramolecular PT. The development of chromic systems by controlling the relative energies of the tautomers in various phases is an active area of research.[3−6] The molecular structure of the OH form of these Schiff bases can be described as a resonance hybrid of a canonical phenol-imine (covalent) form and a protonated quinone-enaminate (ionic) form. As a result of this resonance, intramolecular hydrogen bonding (HB) between the phenol and imine groups is stabilized by electron delocalization over a proton-bridged quasi-six-membered ring. This stabilized HB is called resonance-assisted hydrogen bonding (RAHB),[7,8] although the validity of its nomenclature is still controversial.[9] Recently, the stabilization conferred by RAHB has been recognized as a result of interplay between the substituents and the adjoining π-conjugated system.[10−12] However, the idea that the thermodynamic preference for PT arises from the stabilization of intramolecular HB is questionable, because a strong acid−strong base pair does not always form a strong hydrogen bond. The relative thermodynamic stabilities of the OH and NH forms are considerably influenced by intermolecular interactions both in solution and in the solid state, as well as by their molecular structures.[13−18] For example, Schiff bases of the constitutional isomers 2-hydroxynaphthalene-1-carbaldehyde (α-imine) and 3-hydroxynaphthalene-2-carbaldehyde (β-imine) behave differently from each other with respect to the tautomeric equilibrium in various solvent environments: the α-imine undergoes intramolecular PT much more easily than the β-imine.[19−25] This observation is supported by analysis of Kekulé structures, which can be used to evaluate the trade-off in the NH form between stabilization due to resonance effects and destabilization due to the loss of aromaticity. Clarification of the mechanisms by which intramolecular PT is promoted or inhibited by the adjoining π-conjugated system is necessary. To this end, the probability of PT should be discussed in terms of the relative magnitudes of the effects of RAHB on the OH and NH forms. This analysis of resonance-assisted PT suggests that an appropriately designed π-conjugated system could transmit information about protonation states to adjoining RAHB units.

We have been studying the synthetic and physical organic chemistry of constitutionally isomeric bis(iminomethyl)-2,6-dihydroxynaphthalenes, namely, α,α-diimines **1** and β,β-diimines **2** (Figure 1).[26] These compounds are members of a unique subgroup of double-headed salicylaldehyde analogues that have

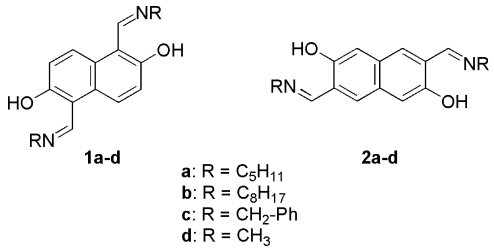

Figure 1. Structures of α,α-diimines **1** and β,β-diimines **2**.

Received: May 21, 2013
Published: August 26, 2013

dx.doi.org/10.1021/jo401108z | J. Org. Chem. 2013, 78, 9021−9031

been extensively studied because they can be used to create a variety of macrocyclic and polymeric Schiff bases and their associated transition-metal complexes.[27−34] For example, we have recently developed a series of fused oligosalphen complexes of some transition metals.[35] Studies of the interplay between the π-conjugated system and the HB units can be expected to contribute to our understanding of the chemistry of analogous coordination compounds that would have interesting functions originating in an interplay between the metal ion and the ligand's π-conjugated system.[36−40] In this paper, we describe our experimental and theoretical studies of resonance effects on intramolecular HB and PT in double-headed salicylaldimines **1** and **2**, which consist of two proton-bridged quasi-six-membered rings that are connected by an identical π-conjugated system but have different connection topologies. We discuss the mechanism of mutual interference between the intramolecular PT sites through the adjoining π-conjugated system. Although we confine our discussion to PT in the thermally equilibrated systems, excited-state intramolecular PT is also an important topic in photophysical chemistry research.[41]

RESULTS AND DISCUSSION

Solution-State Analyses. We prepared α,α-diimines **1** and β,β-diimines **2** from constitutionally isomeric 2,6-dihydroxynaphthalenedicarbaldehydes[26] by condensation with appropriate amines. On the basis of the molecular structures of **1** and **2**, we can postulate three tautomers for each compound, namely, the OH/OH, NH/OH, and NH/NH forms with respect to the two salicylaldimine moieties (Scheme 1). The three tautomers of **1** are hereafter denoted as $\mathbf{1}_{OH/OH}$, $\mathbf{1}_{NH/OH}$, and $\mathbf{1}_{NH/NH}$, respectively. The ^{1}H NMR spectrum of **1a** in DMSO-d_6 showed a doublet at 9.24 ppm (^3J = 4.8 Hz) attributable to the azomethine protons and a broad singlet at 14.87 ppm attributable to an OH or NH proton. The appreciable vicinal coupling between these protons indicates the presence of $\mathbf{1}_{NH/OH}$ or $\mathbf{1}_{NH/NH}$,[24,25] but evaluating the equilibrium constant is difficult because the two salicylaldimine moieties may tautomerize individually. In contrast, the ^{1}H NMR spectrum of a $CDCl_3$ solution of **1a** showed relatively sharp singlets at 8.90 and 14.99 ppm, suggesting that the compound existed in the OH form in this less polar solvent. We observed similar differences between NMR spectra for the DMSO and $CDCl_3$ solutions of **1b** and **1c**.

In contrast, the ^{1}H NMR spectrum of **2a** in DMSO-d_6 showed two sharp singlets, at 8.71 ppm (azomethine) and 12.86 ppm (OH), implying that the populations of the NH/OH and NH/NH forms of **2** were negligibly small. Two singlets, at 8.50 and 12.91 ppm, were also observed in the $CDCl_3$ spectrum. These observations suggest that intramolecular PT did not take place to an appreciable extent in **2**, irrespective of the solvent polarity.

The equilibria shown in Scheme 1 were verified by means of UV−vis spectroscopy (Figure 2). The absorption spectra of **1b** and **2b** in methylcyclohexane solution were reminiscent of the spectra of the corresponding dicarbaldehydes, namely, 2,6-dihydroxynaphthalene-1,5-dicarbaldehyde and 3,7-dihydroxynaphthalene-2,6-dicarbaldehyde (Figure S1, Supporting Information). This observation indicates that the absorption bands of **1b** and **2b** measured in this relatively nonpolar solvent were due to the OH/OH forms. In the spectra of **1b** in methylcyclohexane, tetrahydrofuran, and ethanol and various mixtures of these solvents (Figure 2a), the absorption profile between 370 and 500 nm was strongly solvent dependent and consisted of three bands, with peaks at 400, 456, and 481 nm. On the basis of plots of the absorptivity at these wavelengths as a function of the estimated

Scheme 1. Possible Tautomers of α,α-Diimines 1 and β,β-Diimines 2

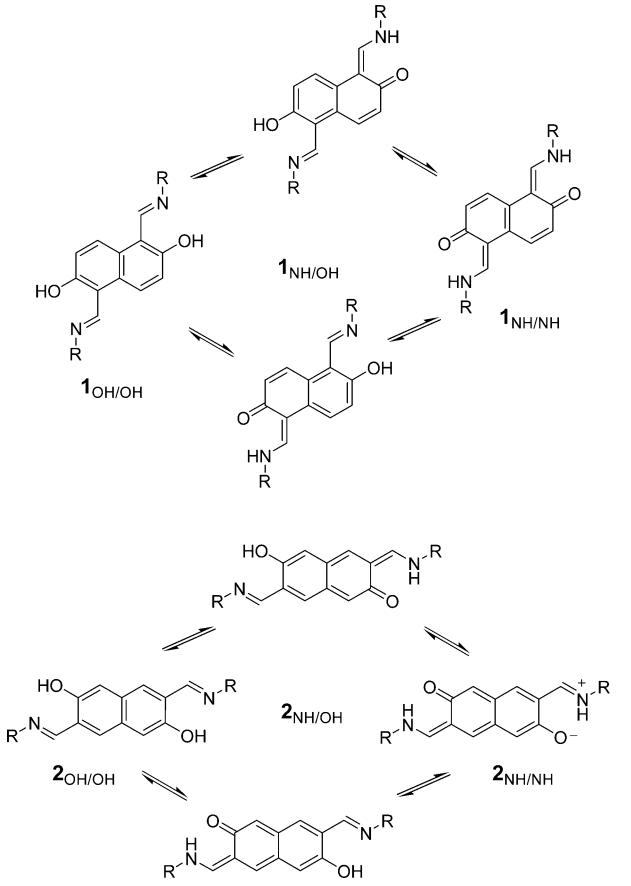

dielectric constants of the solvents (Figure 2a, inset),[42] we attributed these three bands to $\mathbf{1b}_{OH/OH}$, $\mathbf{1b}_{NH/OH}$, and $\mathbf{1b}_{NH/NH}$, respectively. Unlike these bands, the absorption at around 320 nm was less sensitive to the solvent composition. Thus, the former absorptions were assigned to intramolecular charge transfers involving the substituents, whereas the latter was due to transitions innate to the naphthalene moiety.

By means of an arithmetic treatment of the series of solvent-dependent spectra of **1b**, we derived ideal spectra for each tautomer[43] and then reconstituted the spectra to estimate the molar fraction of each tautomer (Figures S2 and S3, Supporting Information). Although peak separation was difficult owing to the lack of an easily recognizable isosbestic point between the spectra of $\mathbf{1b}_{NH/OH}$ and $\mathbf{1b}_{NH/NH}$, the variation of the molar fraction with the solvent polarity seems reasonable from two viewpoints. First, in relatively nonpolar media, the major component was the OH/OH form, in which strong intramolecular hydrogen bonds reduced the polarity of the molecule. Second, as the polarity of the medium was increased, the molar fractions of the NH/OH and NH/NH forms also increased; these tautomers can be thought of as existing in a zwitterionic state. The observed trends were in good agreement with trends observed for similar Schiff bases.[19,21] We judged that the use of a protic solvent, ethanol, had no specific influence on the HB state.[19,22] For $2 < \varepsilon < 7.5$, only a trace of $\mathbf{1b}_{NH/NH}$ was observed. In contrast, in pure ethanol (ε = 25), $\mathbf{1b}_{NH/NH}$ was the major component and the $\mathbf{1b}_{OH/OH}/\mathbf{1b}_{NH/NH}$ and $\mathbf{1b}_{NH/OH}/\mathbf{1b}_{NH/NH}$ population ratios were 0.08 and 0.88, respectively. The difference in solvent composition dependence between $\mathbf{1b}_{NH/OH}$ and

dx.doi.org/10.1021/jo401108z | J. Org. Chem. 2013, 78, 9021−9031

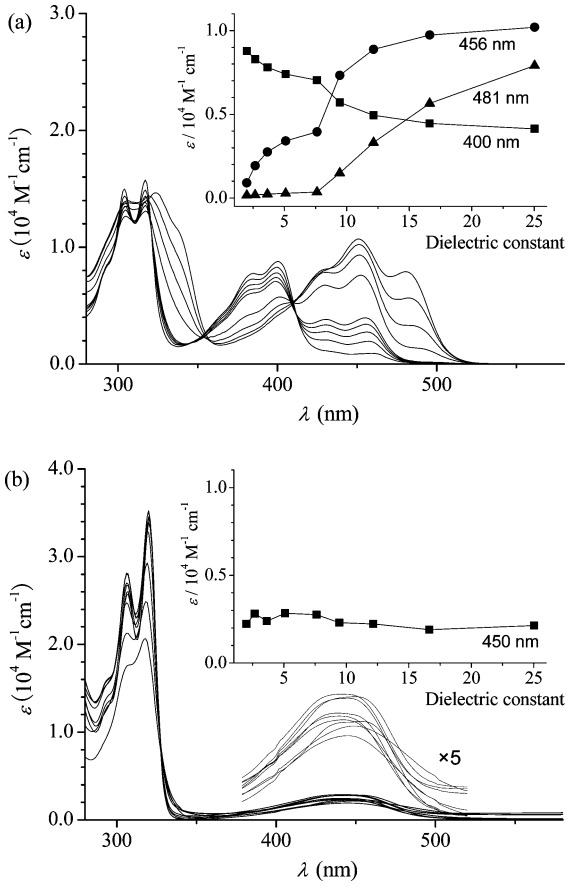

Figure 2. UV−vis absorption spectra of (a) **1b** and (b) **2b** in methylcyclohexane, tetrahydrofuran, ethanol, 75/25, 50/50, and 25/75 mixtures of methylcyclohexane and tetrahydrofuran, and 75/25, 50/50, and 25/75 mixtures of tetrahydrofuran and ethanol. Each inset shows the absorptivity at selected wavelengths as a function of the dielectric constant of the solvents used.

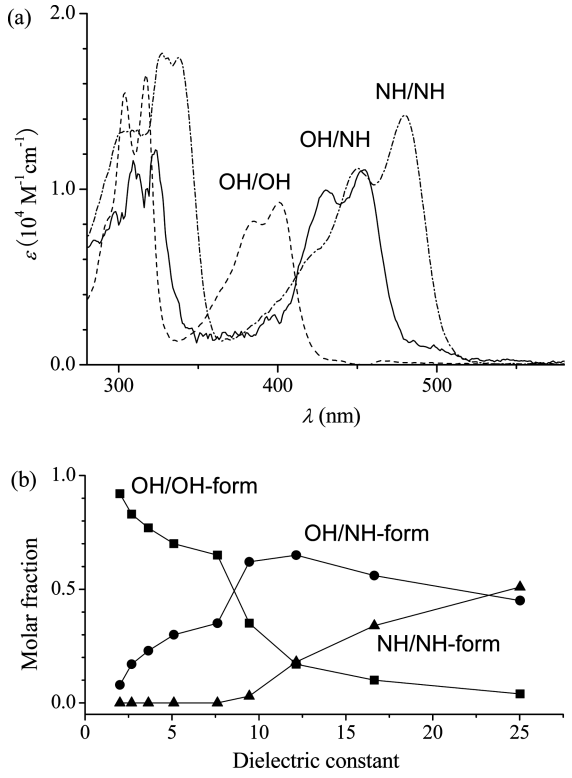

Figure 3. (a) Ideal spectra of the OH/OH, NH/OH, and NH/NH forms of **1b**. (b) Solvent dependence of the molar fraction of each tautomer, calculated on the basis of the ideal spectra.

$\mathbf{1b}_{NH/NH}$ indicates that PT in one of the salicylaldimine groups interfered to some extent with PT in the other.

The UV−vis spectra of **2b** were measured under conditions similar to those used for **1b** (Figure 2b). The spectra consisted of an extremely broadened weak absorption band around 440 nm and an intense absorption band around 320 nm. We attributed these bands to intramolecular charge-transfer transitions and to transitions innate to the naphthalene core, respectively. It is notable that the charge-transfer band for the *β*,*β*-diimine, unlike that of the *α*,*α*-diimine, depended only slightly on the solvent (the band was red-shifted by ∼20 nm as the solvent polarity was increased). Again, this behavior is reminiscent of that of similar compounds reported in the literature.[23] There are two possible explanations for the weak solvatochromism of **2**: (1) the charge-transfer band was intrinsically solvent insensitive or (2) one tautomer predominated at equilibrium. As discussed later, theoretical analysis suggests that the second explanation is the correct one.

Solid-State Analyses. Solid-state UV−vis absorption spectra of **1b** and **2b** were measured at various temperatures in the region of 380−580 nm with an optical microscope equipped with a glass fiber-guided spectrometer (Figure 4).[44] The samples were smeared on a glass substrate, and the thickness of the smeared film was adjusted so that the maximum absorbance was ∼1. The crystallinity of a compound is supposedly maintained after such a sampling procedure, and the orientation of the molecules can be regarded as virtually isotropic. The spectra of **1b** consisted of several peaks attributed to the OH/OH, NH/OH, and NH/NH forms, with reference to the ideal spectra of the tautomers shown in Figure 3. We interpreted the spectrum at 93 K as resulting from overlap of the spectra of the OH/OH (400 and 425 nm) and NH/OH (444 and 478 nm) forms. When the temperature was increased to 273 K, the contribution of the OH/OH form decreased, and the contribution of the NH/NH form (478 and 514 nm) became appreciable. The similarity between the solution- and solid-state spectral profiles suggests that, in the crystal, the NH forms can be symbolically represented as zwitterionic structures, rather than as keto-enamines. The peak maxima in the solid-state spectra were uniformly red-shifted by 20−30 nm compared to the corresponding maxima in the solution-state spectra; we attributed this shift to solid-state effects.[45] At 393 K, the spectral profile was substantially the same as that at 273 K, except for a slight overall blue shift.

Unlike the solid-state spectrum of **1b**, that of **2b** was relatively insensitive to the temperature (Figure 4b). At 93 K, the spectrum showed two well-resolved peaks, at 438 and 462 nm, probably assignable to vibronic structures. As the temperature was increased, the profile broadened, and the absorption maximum (454 nm) was red-shifted by 10−20 nm, which we again attributed to solid-state effects.

Next we investigated the influence of crystal packing on the solid-state absorption spectra of *α*,*α*-diimines **1a**−**c** at 273 K (Figure 5a). Interestingly, the absorption profiles of the three compounds were markedly different from one another, suggesting that the tautomer compositions were different. The intense peak at 520 nm in the spectrum of **1a** indicates a sizable contribution from the NH/NH form, whereas the spectrum of **1c**

dx.doi.org/10.1021/jo401108z | J. Org. Chem. 2013, 78, 9021−9031

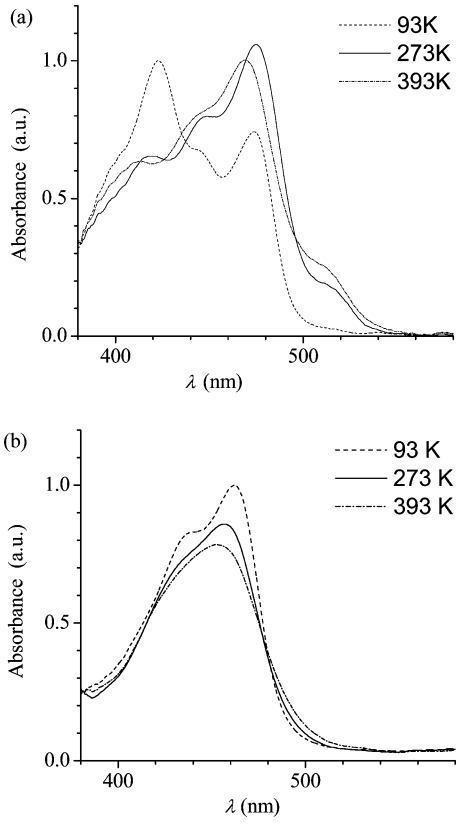

Figure 4. Solid-state UV−vis absorption spectra of smeared film samples of (a) **1b** and (b) **2b** at various temperatures.

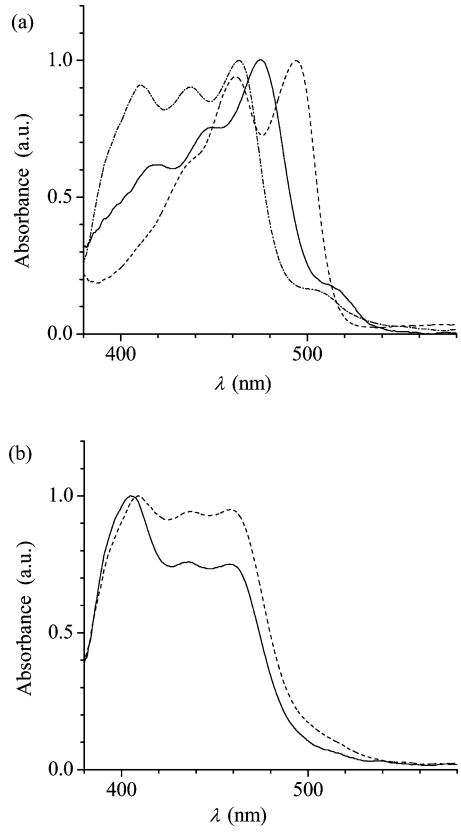

Figure 5. Absorption spectra of **1a** (dashed line), **1b** (solid line), and **1c** (dotted line): (a) smeared solid films at 273 K and (b) molten liquid films (only **1a** and **1b**).

suggested a high content of the OH/OH form. However, the spectra of **1a** and **1b** showed quite similar profiles when they were measured at a temperature slightly higher than the melting point of each compound (Figure 5b). Consequently, the difference in the tautomer composition can be attributed to differences in the molecular packing in the crystals.

Figure 6 shows proximal pairs of molecules in the crystals of **1a−c**. The lengths of the C−O and C−N bonds in **1a** were 1.285 and 1.306 Å, respectively, which are within the typical ranges for NH forms.[13] Differential Fourier analysis suggested that the bridging hydrogen atoms were likely attached to the nitrogen atoms. Each oxygen atom had close contacts with the azomethine and iminomethylene groups of the proximal molecule; the C···O distances were 3.522 and 3.266 Å, respectively. These CH···O hydrogen bonds can be expected to stabilize the NH forms by increasing the basicity of the imino group and the acidity of the hydroxy group.

At 93 K, the lengths of the C−O and C−N bonds of **1b** were 1.334 and 1.285 Å, respectively, which are in the expected ranges for OH forms.[13] Differential Fourier analysis also resulted in definitive positions for the hydrogen atoms attached to oxygen atoms. The naphthalene rings stacked to form columns, and the alkyl chains formed an interdigitated structure among the columns. Each oxygen atom had close contacts with the α-, β-, and γ-carbons of the alkyl chains of the proximal molecule, resulting in C···O distances of 3.335, 3.322 (not indicated in Figure 6b), and 3.409 Å, respectively. This packing structure implies that the oxygen atoms had relatively hydrophobic surroundings, which can be expected to have stabilized the OH forms.

In the structure of **1c**, there were two independent molecules, each of which had a centroid (that is, the two halves of the molecules were asymmetric units). For one molecule, the C−O and C−N bond lengths were 1.335 and 1.288 Å, and for the other molecule, the corresponding bond lengths were 1.324 and 1.286 Å. For convenience, these two molecules are designated A and B. The bond lengths for both molecules were within the typical ranges for OH forms.[13] Differential Fourier analysis suggested that the hydrogen atom was attached to the oxygen atom, although the O−H bond lengths (1.12 and 1.16 Å for molecules A and B, respectively) were somewhat longer than the typical value, and the N−H interatomic distances (1.44 and 1.40 Å) were rather short. These results imply that the HB moiety existed as a proton-bridged six-membered ring. The chemical environments of molecules A and B were similar to each other, and each set of A and B formed an individual HB network, in which the oxygen in the 6-position had a close contact (3.342 Å) with the hydrogen atom in the 3-position of the proximal naphthalene ring. As was the case for **1b**, this type of packing provided the oxygen atoms with hydrophobic surroundings, which may have stabilized the OH forms.

The overall structural distortion relevant to the thermodynamic population of each tautomer can be well represented by the harmonic oscillator model of aromaticity (HOMA) index.[46−49] The HOMA index is a geometrical criterion of local aromaticity and is defined as the normalized variance of the bond lengths with reference to the length optimum for an ideal aromatic system. To evaluate the HOMA index, we used the following equation:

dx.doi.org/10.1021/jo401108z | J. Org. Chem. 2013, 78, 9021−9031

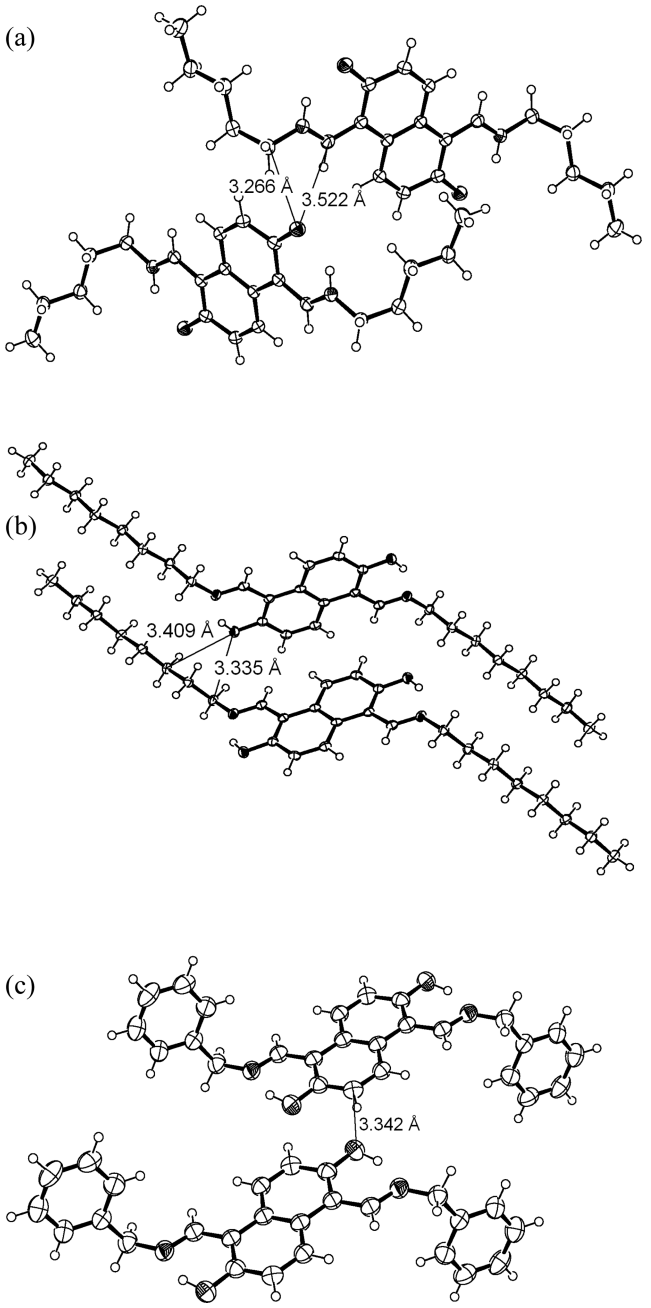

Figure 6. ORTEP drawings of proximal pairs of molecules in the crystal structures of (a) **1a**, (b) **1b**, and (c) **1c**. Selected intermolecular close contacts are shown with interatomic distances. In panel c, only the A molecule is shown for clarity.

$$\mathrm{HOMA} = 1 - \frac{\alpha}{n}\sum_{i=1}^{n}(R_{\mathrm{opt}} - R_i)^2 \qquad (1)$$

where α is a normalization factor, n is the number of constitutive atoms, R_{opt} is a bond length in the optimum structure, and R_i is a bond length in the observed structure. We used R_{opt} = 1.388 Å and α = 257.7, as proposed by Kruszewski and Krygowski.[46] Several studies have shown that the HOMA index correlates well with other geometry-based and magnetism-based criteria of aromaticity.[50−54] The HOMA index for the six-membered rings in the naphthalene moiety of **1a** was 0.53, suggesting that there was a considerable contribution from a less aromatic structure, that is, the NH/NH form, as a result of thermal equilibrium in the packing environment. The HOMA indexes for **1c** were 0.74 and 0.64 for molecules A and B, respectively; these values are close to the HOMA index for the unsubstituted naphthalene system. The HOMA index of **1b** was 0.68, which is close to the average of the two values for **1c**. This significant difference in HOMA indexes predicts that the population of the NH/NH form should increase in the order **1a** > **1b** ≈ **1c**, which is in agreement with the differences in the solid-state absorption spectra of the three compounds (Figure 5a).

The above-described results clearly indicate that the change in crystal packing affected the absorption spectra of **1**, mainly by changing the population of each tautomer. In contrast, the spectra of **2** were relatively insensitive to the temperature, variations in the side chain, or phase transition (Figure S4, Supporting Information). Although the crystal structures of **2a**−**c** have not been determined, we suggest that changes in the microenvironment due to the side chains exerted no substantial effects on the proportion of each tautomer.

Theoretical Analysis. The spectroscopic measurements of **1** and **2** revealed critical differences in various phenomena related to intramolecular PT. To clarify how the connection topology of the π-conjugated system affected intramolecular PT, we performed some quantum chemical calculations on **1d** and **2d**, methyl derivatives of α,α-diimine and β,β-diimine, as representatives of **1** and **2**, respectively. First, we verified the reliability of the calculation method, and then we attempted to estimate the contribution of RAHB to the stability of each tautomer of **1** and **2**. Finally, we attempted another way of decomposing the energetic cost for PT to understand the interplay between the HB sites and the adjoining π-conjugated system with different connection topologies.

We tried various computational methods of approximation and found that density functional theory calculations at the B3LYP/6-311G** level combined with the self-consistent reaction field approximation explained the experimental results reasonably well. The molecular geometry was optimized at the HF/6-311G** level. We calculated the energies of each tautomer of **1** and **2** in the presence or absence of solvent effects (ε = 25, corresponding to ethanol; Table 1). Under in vacuo conditions, the energy increases as each HB site in the OH form is altered to that in the NH form. When solvent effects were incorporated, the energies of $\mathbf{1}_{\mathrm{NH/OH}}$ and $\mathbf{1}_{\mathrm{NH/NH}}$ decreased by ∼15 and ∼30 kJ/mol, respectively; as a result, the relative stabilities of the two tautomers were opposite those observed under in vacuo conditions. We calculated the energetic difference between $\mathbf{1}_{\mathrm{NH/OH}}$ and $\mathbf{1}_{\mathrm{NH/NH}}$ to be 2.18 kJ/mol, and from this value, we

Table 1. Energies of Tautomers of Aldimines Calculated at the B3LYP/6-311G Level**

	energy (kJ/mol)		λ_{max} (nm)		⟨HOMA⟩[a]	
	ε = 1	ε = 25	ε = 1	ε = 25	ε = 1	ε = 25
$\mathbf{1}_{\mathrm{OH/OH}}$	(0.0)	(0.0)	360	358	0.70	0.70
$\mathbf{1}_{\mathrm{NH/OH}}$	+6.9	−7.7	396	396	0.39	0.46
$\mathbf{1}_{\mathrm{NH/NH}}$	+20.4	−9.9	441	446	0.00	0.19
$\mathbf{2}_{\mathrm{OH/OH}}$	(0.0)	(0.0)	431	413	0.78	0.77
$\mathbf{2}_{\mathrm{NH/OH}}$	+45.1	+21.2	599	578	0.36	0.60
$\mathbf{2}_{\mathrm{NH/NH}}$	+89.8	+51.9	950	912	0.67	0.66
$\mathbf{3}_{\mathrm{OH}}$	(0.0)	(0.0)	290	286	0.98	0.98
$\mathbf{3}_{\mathrm{NH}}$	+22.8	+4.2	355	360	0.19	0.46

[a]Harmonic oscillator model of aromaticity index averaged over the two six-membered rings.

dx.doi.org/10.1021/jo401108z | J. Org. Chem. 2013, 78, 9021−9031

calculated the $\mathbf{1}_{NH/OH}/\mathbf{1}_{NH/NH}$ population ratio to be 0.83 (at 298 K) when we correctly included the statistical weight of the tautomers. The $\mathbf{1}_{OH/OH}/\mathbf{1}_{NH/NH}$ population ratio was calculated to be 0.02. These values were in good agreement with the observed values (0.88 and 0.08, respectively); therefore, we concluded that this level of calculation was sufficient.

Solvent effects stabilized $\mathbf{2}_{NH/OH}$ and $\mathbf{2}_{NH/NH}$ to a larger degree (~24 and ~38 kJ/mol, respectively) than they stabilized $\mathbf{1}_{NH/OH}$ and $\mathbf{1}_{NH/NH}$, but the former two tautomers were nevertheless much less stable than $\mathbf{2}_{OH/OH}$. This result suggests that the relative instability of those tautomers was intrinsic to the molecular constitution, rather than the result of the insensitivity of **2** to environmental effects.

We also calculated the absorption wavelengths by means of time-dependent density functional theory at the B3LYP/6-311G** level (Table 1). The calculated absorption maxima for the OH/OH, NH/OH, and NH/NH forms of **1** in vacuo were 359, 396, and 441 nm. The maxima were almost completely insensitive to the solvent polarity, suggesting that the solvent had a minimal effect on the π-electronic states of the tautomers of **1**. The calculated maxima agreed qualitatively with the corresponding observed values (400, 456, and 481 nm) with a systematic displacement of 40−60 nm. The calculated absorption maxima of **2** varied with changes in the protonation state over a wider range (12700 cm^{-1}) than the maxima (5180 cm^{-1}) for **1** and showed substantial solvent dependence. Increasing the solvent polarity caused a blue shift of 20−30 nm for **2**, suggesting that the ground state was more sensitive to the solvent polarity than the excited state. Allowing for a 10−30 nm difference between the observed and calculated values, we confidently assigned the observed absorption maximum at 440 nm to $\mathbf{2}_{OH/OH}$. In summary, the absorption maxima of **1** were moderately tautomer dependent, and the ratio of tautomers was highly solvent dependent. In contrast, the absorption maxima of **2** depended both on the tautomeric form and on the solvent, but the observable tautomer was energetically limited to the OH/OH form in common solvents. These results perfectly explain the observed solvatochromic behavior.

We determined the HOMA indexes for each of the six-membered rings in **1** and **2** to estimate the change in the π-electronic state caused by the change in the protonation state (Figure 7). For **1**, the first and second PTs decreased the HOMA indexes of the adjoining six-membered ring by 0.64 and 0.67 unit, respectively. The HOMA indexes of the six-membered rings farthest from the PT site increased by 0.16 and 0.13 unit, respectively. The PT-induced changes in the HOMA indexes for **2** were completely different from those for **1**. The first and second PTs caused changes of −0.03 and +0.21 unit, respectively, for the adjoining six-membered ring, and changes of −0.32 and +0.08 unit, respectively, for the distant ring.

As a measure of the overall aromaticity of the molecules, we used HOMA indexes averaged over the two six-membered rings, hereafter referred to as ⟨HOMA⟩ indexes. The ⟨HOMA⟩ indexes for all the tautomers of **1** and **2** are listed in Table 1. The ⟨HOMA⟩ indexes were slightly increased by incorporation of solvent effects, especially for the NH-bearing forms, indicating that the NH-bearing forms assumed zwitterionic character in polar environments. The ⟨HOMA⟩ indexes of **1** decreased monotonically with the number of HB sites in the NH form, indicating that the two aromatic rings were virtually independent.[26] In contrast, the ⟨HOMA⟩ indexes of **2** showed no apparent correlation with the number of HB sites in the NH form. For $\mathbf{2}_{NH/OH}$, in contrast to $\mathbf{1}_{NH/OH}$, the HOMA index for

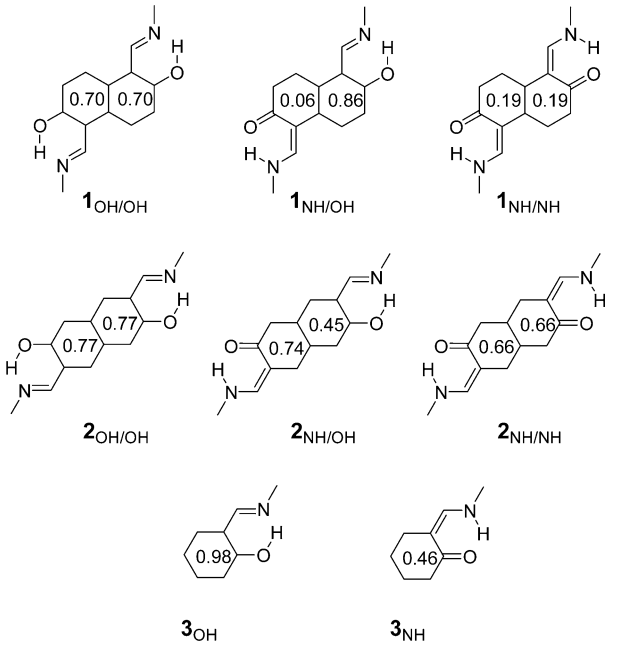

Figure 7. Calculated HOMA indexes for each six-membered ring in the tautomers of **1** and **2**. The structures were optimized with incorporation of solvent effects (ε = 25).

the six-membered ring in the NH form was higher than that of the other ring in the OH form. Furthermore, note that the second PT in $\mathbf{2}_{NH/NH}$ resulted in recovery of aromaticity.

Many other researchers have pointed out that β-imines of naphthols adopt the NH form to a much lesser extent than the analogous α-imines.[19−25] This phenomenon has been explained in terms of a conventional resonance analysis of the energy cost of the loss of aromaticity due to PT: for β-imines, PT reduces the aromaticity of the entire naphthalene ring, whereas for α-imines, only the adjoining six-membered ring is affected. This explanation also applies to **1** and **2**: the PTs at the two intramolecular HB sites in **2** can be expected to have interfered with each other, whereas the PTs were virtually independent in **1**. Resonance hybridization schemes for $\mathbf{1}_{NH/OH}$ and $\mathbf{2}_{NH/OH}$ can explain why the first PT occurred more easily for **1** (in which the left-hand ring retains its aromaticity) than for **2** (in which both rings lose aromaticity) (Scheme 2). The contribution of the zwitterionic structures to $\mathbf{2}_{NH/OH}$ and $\mathbf{2}_{NH/NH}$ was larger than the contribution to $\mathbf{1}_{NH/OH}$ and $\mathbf{1}_{NH/NH}$, which accounts for the theoretical prediction that the energy of **2** should be more sensitive to the solvent polarity than the energy of **1** and the fact

Scheme 2. Resonance Hybridization Schemes for the NH/OH Forms of (a) α,α-Diimines 1 and (b) β,β-Diimines 2

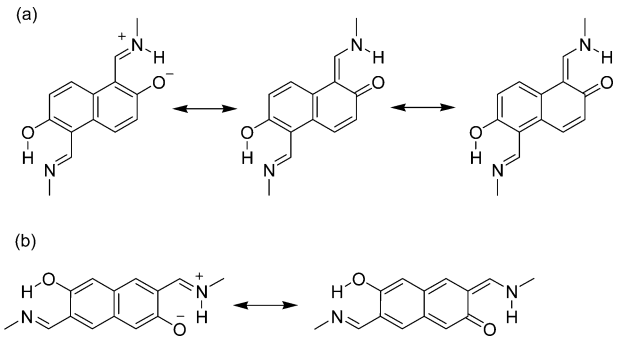

dx.doi.org/10.1021/jo401108z | J. Org. Chem. 2013, 78, 9021−9031

that the absorption maxima were blue-shifted as the solvent polarity was increased. As can be seen from Scheme 2, the large contribution of the ionic structure implies that the aromaticity of the naphthalene core was retained.

We also investigated the origin of (1) the stepwise stabilization of $\mathbf{1}_{NH/OH}$ and $\mathbf{1}_{NH/NH}$ and (2) the intrinsic instability of $\mathbf{2}_{NH/OH}$ and $\mathbf{2}_{NH/NH}$ as compared to the corresponding tautomers of **1**. To directly compare the energies of all the tautomers of **1** and **2**, we considered a hypothetical homodesmotic reaction (Scheme 3).[55] Because these molecules can be considered as formal

Scheme 3. Hypothetical Homodesmotic Reaction for the Formation of *α*,*α*-Diimines 1 and *β*,*β*-Diimines 2

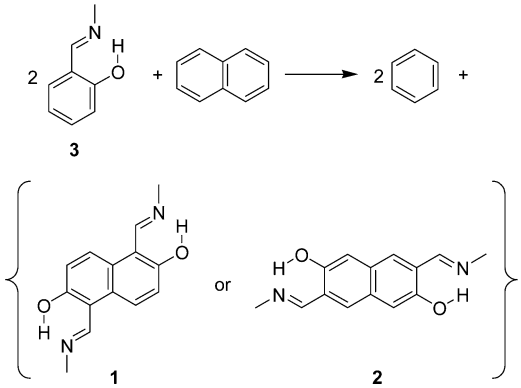

fusions of two salicylaldimine (**3**) units, the enthalpy of the fusion reaction (ΔE_{fusion}) represents the energetic cost of expansion of the conjugated system relative to the energy of naphthalene (E_0; Figure 8). Comparison of the ΔE_{fusion} values calculated for each tautomer (Table 2) reveals that the energetic cost of formal fusion of **1** decreased in the order OH/OH > NH/OH > NH/NH, whereas the sequence for **2** was exactly the opposite. In addition, the ΔE_{fusion} values for **1** varied substantially with the solvent polarity, whereas those for **2** were almost completely

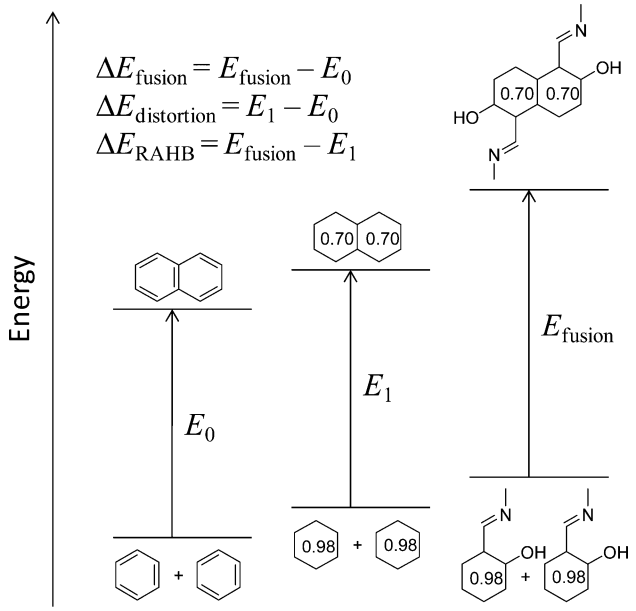

Figure 8. Schematic energy diagram for the homodesmotic reaction shown in Scheme 3.

Table 2. Calculated Energies (kJ/mol) of Tautomers of 1 and 2 Based on the Hypothetical Homodesmotic Reaction Shown in Scheme 3

	ΔE_{fusion}	$\Delta E_{distortion}$	ΔE_{RAHB}
$\mathbf{1}_{OH/OH}$	+28.6	+5.7	+22.9
$\mathbf{1}_{NH/OH}$	+16.7	+6.4	+10.3
$\mathbf{1}_{NH/NH}$	+10.4	+6.3	+4.1
$\mathbf{2}_{OH/OH}$	+13.2	−0.6	+13.8
$\mathbf{2}_{NH/OH}$	+30.2	−7.1	+37.3
$\mathbf{2}_{NH/NH}$	+56.7	−25.3	+82.0

insensitive to solvent effects (data calculated in vacuo are shown in Table S2, Supporting Information).

To a first approximation, ΔE_{fusion} can be simply interpreted as the energetic cost of the π-electron reorganization necessary for formal fusion, and this interpretation seems to agree with the interpretation based on conventional resonance theory. As defined, ΔE_{fusion} is a measure of the loss of aromaticity brought by the formal fusion process. Thus, ΔE_{fusion} might be expected to correlate positively with the total loss of aromaticity. To evaluate this possibility, we calculated the change in the ⟨HOMA⟩ index (referred to as Δ⟨HOMA⟩) relative to the ⟨HOMA⟩ indexes of the constituent salicylaldimine ($\mathbf{3}_{OH}$ or $\mathbf{3}_{NH}$). The Δ⟨HOMA⟩ values for $\mathbf{1}_{OH/OH}$, $\mathbf{1}_{NH/OH}$, and $\mathbf{1}_{NH/NH}$ were −0.28, −0.26, and −0.27 (ε = 25), respectively, whereas the values for $\mathbf{2}_{OH/OH}$, $\mathbf{2}_{NH/OH}$, and $\mathbf{2}_{NH/NH}$ were −0.21, −0.13, and +0.20 (ε = 25), respectively. These values were not correlated either negatively or positively with the ΔE_{fusion} values, implying that, in contrast to the prior assumption, the physical origin of ΔE_{fusion} contributed significantly to the increase in HB stabilization energy; this increase in energy may have compensated for the destabilization due to the loss of aromaticity.

We assumed that ΔE_{fusion} comprised contributions from structural distortion energy ($\Delta E_{distortion}$) and HB energy (ΔE_{RAHB}), including electronic redistribution caused by the change in structure. To estimate $\Delta E_{distortion}$, we calculated the energy of a naphthalene molecule whose carbon skeleton was kept the same as the skeletons of the *α*,*α*- or *β*,*β*-diimines; similarly, we calculated the energy for a benzene molecule whose carbon skeleton was kept the same as that of salicylideneamine. The difference in energy (E_1) between these distorted molecules reflects the destabilization due to the loss of aromaticity. Then we obtained $\Delta E_{distortion}$ from E_1 by subtracting the corresponding energies of the optimized naphthalene and benzene molecules. As expected, $\Delta E_{distortion}$ was strongly correlated with Δ⟨HOMA⟩ (Figure S5, Supporting Information), supporting the idea that the HOMA index serves as a good energetic measure of aromaticity. The first and second PTs in **1** slightly destabilized the aromatic ring, whereas the first PT in **2** resulted in stabilization. The second PT substantially stabilized the aromatic ring in **2**.

Next we calculated the residual contribution ΔE_{RAHB} (= $\Delta E_{fusion} - \Delta E_{distortion}$), which represents the HB energy for the OH or NH form, both of which are stabilized by adjoining aromatic rings, relative to the HB energy for salicylaldimine. Note that because ΔE_{RAHB} reflects several steric effects originating in proximate substituents on the aromatic rings, direct comparison of the absolute values for **1** and **2** is not meaningful. The data listed in Table 2 suggest that the stability of $\mathbf{1}_{NH/OH}$ and $\mathbf{1}_{NH/NH}$ was due to stabilization by RAHB and that the distortion of the aromatic rings made only a minor contribution. In contrast, the instability of $\mathbf{2}_{NH/OH}$ and $\mathbf{2}_{NH/NH}$

dx.doi.org/10.1021/jo401108z | J. Org. Chem. 2013, 78, 9021−9031

was a result of competition between the restoration of aromaticity and the destabilization of the intramolecular HB sites.

As for the strength of intramolecular HB in salicylaldehyde derivatives, we should mention a simple yet sophisticated method for evaluating the relative energies of (I) closed and (II) open conformers.[56] We calculated the energy difference between the open and closed conformers ($\Delta E_{O/C}$) by subtracting the energy of the I form from that of the II form. Then we separated $\Delta E_{O/C}$ into contributions from the putative HB energy (ΔE_{HB}) and the resonance-assistance energy (ΔE_{RA}), according to Grabowski's scheme: $\Delta E_{O/C} = \Delta E_{HB} + \Delta E_{RA}$.[56] The ΔE_{RA} value is the difference in energy between the I form and a structure in which the OH proton has been allowed to hydrogen bond with the imine group and the residual part of the molecule is kept identical to that of the II form. For the double-headed salicylaldimines in the OH/OH form, there are three conformers (I-I, I-II, and II-II), and they are involved in an isodesmic reaction (Scheme S1, Supporting Information) that is affected by the orientation of the OH group(s) on the naphthalene core.[26] Table S1 (Supporting Information) summarizes the results of energy-decomposition analyses of these conformers of **1** and **2**. In contrast to the energy of the OH···N bond in the OH form, the energy of the NH···O bond in the NH form is difficult to estimate, because the comparison of the open and closed conformers is not applicable to this case. Therefore, we cannot directly evaluate the resonance effect on the HB energy in the NH-bearing form by means of a method similar to Grabowski's method. From the $\Delta E_{HB} + \Delta E_{RA}$ values (50−70 kJ/mol), we can safely say only that the ΔE_{RAHB} values in Table 2 are within a reasonable range.

We attempted to gain insight into the essential factors determining the probability of intramolecular PT. The experimental and theoretical results highlight a crucial difference between the probabilities of PT in **1** and **2**, suggesting that the stability of the NH form relative to that of the OH form was strongly affected by the connection topology of the adjoining π-conjugated system. By drawing an analogy with the energetic contributions to $\Delta E_{O/C}$,[56] we assumed that the energy (ΔE_{PT}) of PT can be divided into two contributions: (1) the difference between the dissociation energies of the OH group and the N^+H group and (2) structural changes and electronic redistribution. Here, ΔE_{PT} is defined as the energy of the NH form relative to that of the OH form. The first contribution originates from a putative acid−base reaction ($\Delta E_{acid-base}$), and the second contribution originates from the relaxation of the adjacent π-conjugated system ($\Delta E_{relaxation}$, Figure 9).

The energy of PT (ΔE_{PT}) was calculated from the values in Table 3. The energy of the acid−base reaction ($\Delta E_{acid-base}$) is the change in energy due to the change in the connectivity of the hydrogen atom when the geometry of the rest of the molecule remains unchanged. We derived the energy for the structural relaxation ($\Delta E_{relaxation}$) as $\Delta E_{PT} - \Delta E_{acid-base}$. Table 3 summarizes the calculated energies, which highlight the difference between **1** and **2** with respect to the contributions of ΔE_{PT}. The values in Table 3 were calculated under solvated conditions; for reference, in Table S3 (Supporting Information), the values are compared with the corresponding values calculated under in vacuo conditions. There were considerable differences among the values of $\Delta E_{relaxation}$, which varied from −20 to −40 kJ/mol. For all the PTs examined, the putative acid−base reactions were endothermic, although the $\Delta E_{acid-base}$ values ranged from 20 to 50 kJ/mol depending on the structure of the molecule. The $\Delta E_{acid-base}$ value of the first PT for **1** was ∼30 kJ/mol, which is almost the same as that for **3**; whereas the value for **2** (40 kJ/mol) was significantly higher than that for **3**. For the second PT, the $\Delta E_{acid-base}$ value for **1** was 10 kJ/mol less than that for the first PT. In contrast, the corresponding value for **2** was 10 kJ/mol larger than that for the first PT. That is, from the perspective of the putative acid−base reaction, the first PT promoted the second PT for **1**, whereas the first PT suppressed the second PT for **2**. Using the values in Table 3, we plotted approximate quadratic potential curves for the energies of the tautomers of **1** and **2** versus the square root of 1 − ⟨HOMA⟩, which is a geometrical parameter related to the loss of aromaticity (Figure 10).

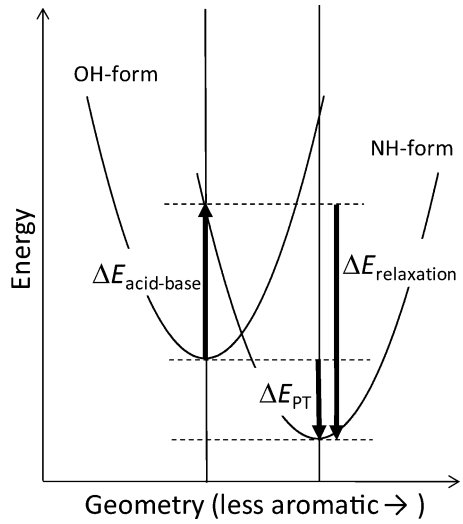

Figure 9. Theoretical potential curves of OH and NH forms as a function of a geometrical index of aromaticity. Energies related to intramolecular proton transfer are indicated by arrows.

Table 3. Calculated Energies (kJ/mol) Related to Intramolecular Proton Transfer

	ΔE_{PT}	$\Delta E_{acid-base}$	$\Delta E_{relaxation}$
$\mathbf{1}_{OH/OH} \rightarrow \mathbf{1}_{NH/OH}$	−7.7	+29.4	−37.1
$\mathbf{1}_{NH/OH} \rightarrow \mathbf{1}_{NH/NH}$	−2.2	+22.0	−24.2
$\mathbf{2}_{OH/OH} \rightarrow \mathbf{2}_{NH/OH}$	+21.2	+43.1	−21.9
$\mathbf{2}_{NH/OH} \rightarrow \mathbf{2}_{NH/NH}$	+30.7	+52.4	−21.8
$\mathbf{3}_{OH} \rightarrow \mathbf{3}_{NH}$	+4.2	+30.9	−26.7

These curves highlight the differences in how the structural displacement influences the energies of **1** and **2**. On one hand, PT in **1** caused a loss of aromaticity, and electronic stabilization of the protonation state overwhelmed the destabilization due to structural distortion. On the other hand, PT in **2** also caused a loss of aromaticity, but the destabilization due to structural distortion overwhelmed the electronic stabilization of the protonation state. Consequently, in **2**, the retention of aromaticity took precedence over the stabilization of the protonation state, resulting in a phenomenon totally opposite that of **1**; namely, HB is not assisted by resonance effects from the adjoining aromatic ring. This difference is due solely to the connection topology of the two salicylaldimine moieties fused into the naphthalene ring system. It is interesting that high-level quantum chemical calculations gave a quantitative reason for the conventional picture obtained by drawing simple Kekulé structures in resonance hybridization schemes.

dx.doi.org/10.1021/jo401108z | J. Org. Chem. 2013, 78, 9021−9031

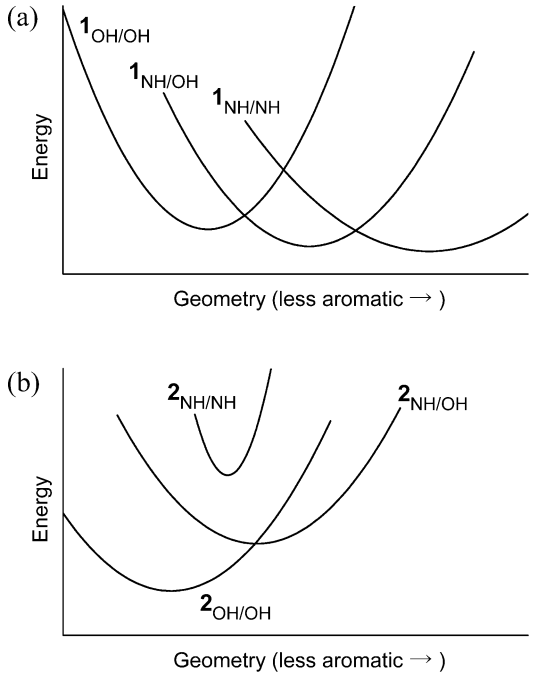

Figure 10. Approximate quadratic potential curves for the tautomers of (a) **1** and (b) **2**. Energy is plotted against a geometrical parameter related to the loss of aromaticity.

CONCLUSIONS

We prepared diimine derivatives of *α,α*- and *β,β*-dicarbaldehydes of 2,6-dihydroxynaphthalene and examined their tautomerization behavior on the basis of the idea that these molecules can be regarded as fused salicylaldimines. The tautomeric equilibrium of the *α,α*-diimines was strongly influenced by the solvent polarity, temperature, and crystal packing. In contrast, prototopic tautomerization of the *β,β*-diimines was barely affected by changes in the molecular environment. Quantum chemical calculations revealed the origin of the difference in tautomerization behavior between these constitutional isomers. Several energy decomposition analyses indicated a fundamental difference in the electronic states of the molecules, a difference that originated in the connection topology of the two salicylaldimine moieties fused into the naphthalene ring system. We concluded that, for the *α,α*-diimines, the NH forms were substantially stabilized by RAHB, and distortion of the aromatic rings made only a small contribution. In contrast, for the *β,β*-diimines, stabilization by RAHB exacted a high energetic price due to structural distortion (loss of aromaticity). As a result of competition between restoration of aromaticity and destabilization of HB sites, the *β,β*-diimines exclusively adopted the OH/OH form.

EXPERIMENTAL SECTION

Synthesis. *1,5-Bis(iminomethyl)-2,6-dihydroxynaphthalenes **1a–c**.* According to the reported procedure,[26] 1,5-diformyl-2,6-dihydroxynaphthalene (**3**) was prepared. A 2 equiv (2.0 mmol) portion of pentylamine (0.174 g), octylamine (0.258 g), or benzylamine (0.214 g) was added to a methanol suspension of **3** (0.216g, 1.0 mmol), which immediately turned to a clear yellow solution, and afterward, crystalline solids were separated out at ambient temperature. The product was collected by filtration and dried under reduced pressure at 25 °C.

Data for **1a** (pentylamine derivative): orange prisms (yield 0.28 g, 79%); mp 146—147 °C; IR (KBr) 1631 cm^{-1} ($\nu_{C=N}$); precise MS (FAB+) m/z 355.2383 (calcd for M + H^+ 355.2385); ^1H NMR ($CDCl_3$) δ = 0.93 (t (J = 7.3 Hz), 6H), 1.33−1.46 (mult, 8H), 1.75 (quint (J = 7.3 Hz), 4H), 3.65 (t (J = 6.8 Hz), 4H), 7.08 (d (J = 9.3 Hz), 2H), 7.98 (d (J = 9.3 Hz), 2H), 8.90 (br s, 2H), 15.00 (br s, 2H); ^{13}C NMR ($CDCl_3$) δ = 14.0, 22.4, 29.2, 30.6, 56.2, 109.2, 123.3, 125.3, 126.2, 159.3, 167.7.

Data for **1b** (octylamine derivative): orange needles (yield 0.42 g, 96%); mp 136—137 °C; IR (KBr) 1632 cm^{-1} ($\nu_{C=N}$); MS (FAB+) m/z 439.5 (calcd for M + H^+ 439.33); ^1H NMR ($CDCl_3$) δ = 0.88 (t (J = 6.9 Hz), 6H), 1.28−1.46 (mult, 20H), 1.75 (quint (J = 7.1 Hz), 4H), 3.65 (t (J = 7.1 Hz), 4H), 7.08 (d (J = 9.4 Hz), 2H), 7.98 (d (J = 9.4 Hz), 2H), 8.90 (br s, 2H), 15.00 (br s, 2H), ^{13}C NMR ($CDCl_3$) δ = 14.1, 22.6, 27.0, 29.2, 29.3, 30.9, 31.8, 56.3, 109.2, 123.3, 125.3, 126.1, 159.3, 167.7. Anal. Calcd for $C_{28}H_{42}N_2O_2$: C, 76.67; H, 9.65; N, 6.39. Found: C, 76.71; H, 9.75; N, 6.17.

Data for **1c** (benzylamine derivative): orange platelets (yield 0.38 g, 96%); mp not observed (dec < 300 °C); IR (KBr) 1625 cm^{-1} ($\nu_{C=N}$); precise MS (FAB+) m/z 395.1750 (calcd for M + H^+ 395.1759); ^1H NMR (DMSO-d_6) δ = 4.91 (s, 4H), 7.00 (d (J = 9.4 Hz), ArH, 2H), 7.30−7.35 (mult, 2H), 7.38−7.42 (mult, 8H), 8.32 (d (J = 9.4 Hz), 2H), 9.49 (d (J = 3.7 Hz), 2H), 14.89 (br s, 2H); ^{13}C NMR spectra could not be measured due to low solubility.

*3,7-Bis(iminomethyl)-2,6-dihydroxynaphthalenes **2a–c**.* According to the reported procedure,[26] 3,7-diformyl-2,6-dihydroxynaphthalene (**4**) was prepared. A 2 equiv (2.0 mmol) portion of pentylamine (0.174 g), octylamine (0.258 g), or benzylamine (0.214 g) was added to a methanol suspension of **4** (0.216g, 1.0 mmol), which immediately turned to a clear yellow solution, and afterward, crystalline solids were separatred out at ambient temperature. The product was collected by filtration and dried under reduced pressure at 25 °C.

Data for **2a** (pentylamine derivatives): yellow needles (yield 0.26 g, 74%); mp 264—265 °C (dec after melt); IR (KBr) 1643 cm^{-1} ($\nu_{C=N}$); precise MS (FAB+) m/z 355.2395 (calcd for M + H^+ 355.2385); ^1H NMR ($CDCl_3$) δ = 0.92 (t (J = 7.2 Hz), 6H), 1.35−1.41 (mult, 8H), 1.73 (quint (J = 7.2 Hz), 4H), 3.65 (t (J = 6.8 Hz), 4H), 7.23 (s, 2H), 7.65 (s, 2H), 8.50 (s, 2H), 12.90 (br s, 2H); ^{13}C NMR ($CDCl_3$) δ = 14.1, 22.5, 29.4, 30.4, 60.2, 111.1, 123.1, 129.3, 130.8, 155.0, 164.5.

Data for **2b** (octylamine derivatives): yellow needles (yield 0.41 g, 94%); mp 230—231 °C; IR (KBr) 1641 cm^{-1} ($\nu_{C=N}$); MS (FAB+) m/z 439.4 (calcd for M + H^+ 439.33); ^1H NMR ($CDCl_3$) δ = 0.88 (t (J = 6.9 Hz), 6H), 1.27−1.44 (mult, 20H), 1.73 (quint (J = 7.3 Hz), 4H), 3.65 (t (J = 6.9 Hz), 4H), 7.23 (s, 2H), 7.65 (s, 2H), 8.50 (s, 2H), 12.90 (br s, 2H); ^{13}C NMR ($CDCl_3$) δ = 14.1, 22.7, 27.2, 29.2, 29.3, 30.8, 31.8, 60.2, 111.0, 123.1, 129.3, 130.8, 155.0, 164.4. Anal. Calcd for $C_{28}H_{42}N_2O_2$: C, 76.67; H, 9.65; N, 6.39. Found: C, 76.40; H, 9.67; N, 6.28.

Data for **2c** (benzylamine derivatives): yellow platelets (recrystallized from DMSO, yield 0.25 g, 64%); mp 290—291 °C (dec after melt); IR (KBr) 1644 cm^{-1} ($\nu_{C=N}$); MS (FAB+) m/z 395.1 (calcd for M + H^+ 395.18); ^1H NMR (DMSO-d_6) δ = 4.89 (s, 4H), 7.27 (s, 2H), 7.30−7.34 (mult, 2H), 7.36−7.40 (mult, 8H), 8.00 (s, 2H), 8.87 (s, 2H), 12.67 (s, 2H); ^{13}C NMR spectra could not be measured due to low solubility. Anal. Calcd for $C_{26}H_{22}N_2O_2 \cdot 0.25H_2O$: C, 78.27; H, 5.68; N, 7.02. Found: C, 78.36; H, 5.64; N, 6.85.

Crystallographic Data. For X-ray diffraction of single crystals, data were collected on diffractometers, λ(Cu Kα) = 1.5418 Å (for **1a** and **1c**) and λ(Mo Kα) = 0.71075 Å (for **1b**). The structure was solved by direct methods and expanded using Fourier techniques. All calculations were performed with the crystallographic software package SHELX-97.[57] Crystallographic data have been deposited with the Cambridge Crystallographic Data Centre: deposition numbers CCDC-939325 to CCDC-939327 for compounds **1a**, **1b**, and **1c**. Copies of the data can be obtained free of charge via http://www.ccdc.cam.ac.uk/conts/retrieving.html (or from the Cambridge Crystallographic Data Centre, 12 Union Rd., Cambridge CB2 1EZ, U.K.; fax +44 1223 336033; e-mail deposit@ccdc.cam.ac.uk).

Data for **1a**: $C_{22}H_{30}N_2O_2$, M_w = 354.48, monoclinic, a = 8.638(1) Å, b = 11.502(1) Å, c = 9.890(1) Å, β = 101.376(2)°, V = 963.36(17) $Å^3$, D_{calcd} = 1.222 g/cm^3, T = 193 K, space group $P2_1/n$ (No. 14), Z = 2, μ(Cu Kα) = 6.1 cm^{-1}, 9088 reflections measured and 1720 unique reflections ($2\theta_{max}$ = 145.9°, R_{int} = 0.024), which were used in all calculations, R = 0.053, R_w = 0.143.

dx.doi.org/10.1021/jo401108z | J. Org. Chem. 2013, 78, 9021−9031

Data for **1b**: $C_{28}H_{42}N_2O_2$, M_w = 438.64, monoclinic, a = 49.85(5) Å, b = 4.657(5) Å, c = 10.848(11) Å, β = 99.408(14)°, V = 2485(4) Å^3, D_{calcd} = 1.173 g/cm^3, T = 93 K, space group $C2/c$ (No. 15), Z = 4, μ(Mo Kα) = 0.73 cm^{-1}, 7380 reflections measured and 1707 unique reflections ($2\theta_{max}$ = 55.0°, R_{int} = 0.039), which were used in all calculations, R = 0.054, R_w = 0.161.

Data for **1c**: $C_{26}H_{22}N_2O_2$, M_w = 394.46, triclinic, a = 9.168(1) Å, b = 10.975(1) Å, c = 11.722(1) Å, α = 65.579(2)°, β = 70.746(2)°, γ = 70.183(2)°, V = 985.28(16) Å^3, D_{calcd} = 1.330 g/cm^3, T = 193 K, space group $P\bar{1}$ (No. 2), Z = 2, μ(Cu Kα) = 6.7 cm^{-1}, 8762 reflections measured and 3474 unique reflections ($2\theta_{max}$ = 146.5°, R_{int} = 0.044), which were used in all calculations, R = 0.088, R_w = 0.366.

Computational Details. The geometry of the molecules was optimized by means of the Hartree−Fock method using the 6-311G** basis set. Since the optimized structure has not been obtained for $\mathbf{2}_{NH/NH}$ under the default criteria of convergence, we adopted the structure obtained under looser criteria (with the Opt=Loose keyword) limitedly for this case. The structure optimized under in vacuo conditions was used as an initial structure for geometrical optimization incorporating solvent effects (ε = 25, assuming ethanol) using the SCRF keyword. The structures thus obtained were used for DFT (B3LYP) calculations using the 6-311G** basis set. All the calculations were performed with the Gaussian 03[58] and Gaussian 09[59] programs.

■ ASSOCIATED CONTENT

Supporting Information

General procedures of the experiments, supplementary figures, schemes, and tables, ^{1}H and ^{13}C NMR spectra of new compounds (**1a−c**, **2a−c**), crystallographic information format (CIF) files for **1a−c**, and numerical data for ab initio calculations. This material is available free of charge via the Internet at http://pubs.acs.org.

■ AUTHOR INFORMATION

Corresponding Author

*E-mail: houjou@iis.u-tokyo.ac.jp. Phone: +81(3)5452 6367. Fax: +81(3)5452 6366.

Notes

The authors declare no competing financial interest.

■ ACKNOWLEDGMENTS

A part of this work (crystallography of **1b**) was conducted in Research Hub for Advanced Nano Characterization, The University of Tokyo, supported by the Ministry of Education, Culture, Sports, Science and Technology (MEXT), Japan.

■ REFERENCES

(1) (a) Cohen, M. D.; Schmidt, G. M. J. *J. Phys. Chem.* **1962**, *66*, 2442. (b) Hadjoudis, E.; Vittorakis, M.; Moustakali-Mavridis, I. *Tetrahedron* **1987**, *43*, 1345.

(2) For reviews, see: (a) Hadjoudis, E. *Mol. Eng.* **1995**, *5*, 301. (b) Hadjoudis, E.; Mavridis, I. M. *Chem. Soc. Rev.* **2004**, *33*, 579. (c) Minkin, V. I.; Tsukanov, A. V.; Dubonosov, A. D.; Bren, V. A. *J. Mol. Struct.* **2011**, *998*, 179.

(3) Yelamaggad, C. V.; Achalkumar, A. S.; Rao, D. S. S.; Prasad, S. K. *J. Org. Chem.* **2009**, *74*, 3168.

(4) Chen, P.; Lu, R.; Xue, P.; Xu, T.; Chen, G.; Zhao, Y. *Langmuir* **2009**, *25*, 8395.

(5) Haneda, T.; Kawano, M.; Kojima, T.; Fujita, M. *Angew. Chem., Int. Ed.* **2007**, *46*, 6643.

(6) (a) Robert, F.; Naik, A. D.; Tinant, B.; Robiette, R.; Garcia, Y. *Chem.—Eur. J.* **2009**, *15*, 4327. (b) Robert, F.; Naik, A. D.; Hidara, F.; Tinant, B.; Robiette, R.; Wouters, J.; Garcia, Y. *Eur. J. Org. Chem.* **2010**, 621.

(7) Gilli, G.; Bellucci, F.; Ferretti, V.; Bertolasi, V. *J. Am. Chem. Soc.* **1989**, *111*, 1023.

(8) (a) Martyniak, A.; Majerz, I.; Filarowski, A. *RSC Adv.* **2012**, *2*, 8135. (b) Filarowski, A.; Koll, A.; Sobczyk, L. *Curr. Org. Chem.* **2009**, *13*, 172. (c) Filarowski, A.; Kochel, A.; Kulba, M.; Kamounah, F. S. *J. Phys. Org. Chem.* **2008**, *21*, 939.

(9) (a) Sanz, P.; Mó, O.; Yáñez, M.; Elguero, J. *ChemPhysChem* **2007**, *8*, 1950. (b) Sanz, P.; Mó, O.; Yáñez, M.; Elguero, J. *J. Phys. Chem. A* **2007**, *111*, 3585. (c) Sanz, P.; Mó, O.; Yáñez, M.; Elguero, J. *Chem.—Eur. J.* **2008**, *14*, 4225.

(10) Sobczyk, L.; Grabowski, S. J.; Krygowski, T. M. *Chem. Rev.* **2005**, *105*, 3513.

(11) (a) Krygowski, T. M.; Zachara-Horeglad, J. E.; Palusiak, M.; Pelloni, S.; Lazzeretti, P. *J. Org. Chem.* **2008**, *73*, 2138. (b) Krygowski, T. M.; Zachara-Horeglad, J. E.; Palusiak, M. *J. Org. Chem.* **2010**, *75*, 4944.

(12) (a) Jezierska-Mazzarello, A.; Panek, J. J.; Szatyłowicz, H.; Krygowski, T. M. *J. Phys. Chem. A* **2012**, *116*, 460. (b) Jezierska-Mazzarelo, A.; Szatyłowicz, H.; Krygowski, T. M. *J. Mol. Model.* **2012**, *18*, 127.

(13) (a) Ogawa, K.; Kasahara, Y.; Ohtani, Y.; Harada, J. *J. Am. Chem. Soc.* **1998**, *120*, 7107. (b) Ogawa, K.; Harada, J.; Tamura, I.; Noda, Y. *Chem. Lett.* **2000**, 528.

(14) Chong, J. H.; Sauer, M.; Patric, O.; MacLachlan, M. J. *Org. Lett.* **2003**, *5*, 3823.

(15) (a) Karabıyık, H.; Ocak-İskeleli, N.; Petek Çiğdem Albayrak, H.; Ağar, E. *J. Mol. Struct.* **2008**, *873*, 130. (b) Karabıyık, H.; Petek, H.; Ocak-İskeleli, N. *Struct. Chem.* **2009**, *20*, 1055.

(16) Pizzala, H.; Carles, M.; Stone, W. E. E.; Thevand, A. *J. Mol. Struct.* **2000**, *526*, 261.

(17) Užarević, K.; Rubčić, M.; Stilinović, V.; Kaitner, B.; Cindrić, M. *J. Mol. Struct.* **2010**, *984*, 232.

(18) Dominiak, P. M.; Grech, E.; Barr, G.; Teat, S.; Mallinson, P.; Woźniak, K. *Chem.—Eur. J.* **2003**, *9*, 963.

(19) (a) Antonov, L.; Fabian, W. M. F.; Nedeltchva, D.; Kamounah, F. S. *J. Chem. Soc., Perkin Trans. 2* **2000**, 1173. (b) Fabian, W. M. F.; Antonov, L.; Nedeltcheva, D.; Kamounah, F. S.; Taylor, P. J. *J. Phys. Chem. A* **2004**, *108*, 7603. (c) Nagy, P. I.; Fabian, W. M. F. *J. Phys. Chem. B* **2006**, *110*, 25026.

(20) Dobosz, R.; Skotnicka, A.; Rozwadowski, Z.; Dziembowska, T.; Gawinecki, R. *J. Mol. Struct.* **2010**, *979*, 194.

(21) Oshima, A.; Momotake, A.; Arai, T. *J. Photochem. Photobiol., A* **2004**, *162*, 473.

(22) Nazır, H.; Yıldız, M.; Yılmaz, H.; Tahir, M. N.; Ülkü, D. *J. Mol. Struct.* **2000**, *524*, 241.

(23) Fernandez-G, J. M.; del Rio-Portilla, F.; Quiroz-Garcia, B.; Toscano, R. A.; Salcedo, R. *J. Mol. Struct.* **2001**, *561*, 197.

(24) Salman, S. R.; Lindon, J. C.; Farrant, R. D.; Carpenter, T. A. *Magn. Reson. Chem.* **1993**, *31*, 991.

(25) Alarcón, S. H.; Olivieri, A. C.; González-Sierra, M. *J. Chem. Soc., Perkin Trans. 2* **1994**, 1067.

(26) Houjou, H.; Motoyama, T.; Banno, S.; Yoshikawa, I.; Araki, K. *J. Org. Chem.* **2009**, *74*, 520.

(27) For reviews, see: (a) Borisova, N. E.; Reshetova, M. D.; Ustynyuk, Y. A. *Chem. Rev.* **2007**, *107*, 46. (b) Leung, A. C.; MacLachlan, M. J. *J. Inorg. Organomet. Polym. Mater.* **2007**, *17*, 57. (c) Whiteoak, C. J.; Salassa, G.; Kleij, A. W. *Chem. Soc. Rev.* **2012**, *41*, 622.

(28) (a) Houjou, H.; Lee, S.-K.; Hishikawa, Y.; Nagawa, Y.; Hiratani, K. *Chem. Commun.* **2000**, 2197. (b) Houjou, H.; Tsuzuki, S.; Nagawa, Y.; Hiratani, K. *Bull. Chem. Soc. Jpn.* **2002**, *75*, 831. (c) Houjou, H.; Sasaki, T.; Shimizu, Y.; Koshizaki, N.; Kanesato, M. *Adv. Mater.* **2005**, *17*, 606. (d) Houjou, H.; Shimizu, Y.; Koshizaki, N.; Kanesato, M. *Adv. Mater.* **2003**, *15*, 1458.

(29) (a) Akine, S.; Hashimoto, D.; Saiki, T.; Nabeshima, T. *Tetrahedron Lett.* **2004**, *45*, 4225. (b) Nabeshima, T.; Miyazaki, H.; Iwasaki, A.; Akine, S.; Saiki, T.; Ikeda, C. *Tetrahedron* **2007**, *63*, 3328.

(30) Asato, E.; Chinen, M.; Yoshino, A.; Sakata, Y.; Sugiura, K. *Chem. Lett.* **2000**, 678.

(31) Shimakoshi, H.; Takemoto, H.; Aritome, I.; Hisaeda, Y. *Tetrahedron Lett.* **2002**, *43*, 4809.

(32) Nomura, R.; So, Y.; Izumi, A.; Nishihara, Y.; Yoshino, K.; Masuda, T. *Chem. Lett.* **2001**, 916.

(33) (a) Hui, J. K.-H.; MacLachlan, M. J. *Chem. Commun.* **2006**, 2480–2482. (b) Gallant, A. J.; Hui, J. K.-H.; Zahariev, F. E.; Wang, Y. A.; MacLachlan, M. J. *J. Org. Chem.* **2005**, *70*, 7936. (c) Gallant, A.; Yun, M.; Sauer, M.; Yeung, C. S.; MacLachlan, M. J. *Org. Lett.* **2005**, *7*, 4827.
(34) (a) Dai, Y.; Katz, T. J. *J. Org. Chem.* **1997**, *62*, 1274. (b) Dai, Y.; Katz, T. J.; Nicholas, D. A. *Angew. Chem., Int. Ed. Engl.* **1996**, *35*, 2109.
(35) (a) Houjou, H.; Motoyama, T.; Araki, K. *Eur. J. Inorg. Chem.* **2009**, 533. (b) Houjou, H.; Ito, M.; Araki, K. *Inorg. Chem.* **2009**, *48*, 10703. (c) Houjou, H.; Ito, M.; Araki, K. *Inorg. Chem.* **2011**, *50*, 5298. (d) Yagi, K.; Ito, M.; Houjou, H. *Macromol. Rapid Commun.* **2012**, *33*, 540.
(36) For reviews, see: (a) Evangelio, E.; Ruiz-Molina, D. *Eur. J. Inorg. Chem.* **2005**, 2957. (b) Sato, O.; Tao, J.; Zhang, Y.-Z. *Angew. Chem., Int. Ed.* **2007**, *46*, 2152. (c) Lemaire, M. T. *Pure Appl. Chem.* **2011**, *83*, 141.
(37) (a) Rotthaus, O.; Thomas, F.; Jarjayes, O.; Philouze, C.; Saint-Aman, E.; Pierre, J.-L. *Chem.—Eur. J.* **2006**, *12*, 6953. (b) Rotthaus, O.; Jarjayes, O.; Thomas, F.; Philouze, C.; Saint-Aman, E.; Pierre, J.-L. *Dalton Trans.* **2007**, 889. (c) Rotthaus, O.; Jarjayes, O.; Philouze, C.; Del Valle, C. P.; Thomas, F. *Dalton Trans.* **2009**, 1792. (d) Arora, H.; Philouze, C.; Jarjayes, O.; Thomas, F. *Dalton Trans.* **2010**, *39*, 10088. (e) Rotthaus, O.; Jarjayes, O.; Thomas, F.; Philouze, C.; del Valle, C. P.; Saint-Aman, E.; Pierre, J.-L. *Chem.—Eur. J.* **2006**, *12*, 2293.
(38) (a) Shimazaki, Y.; Tani, F.; Fukui, K.; Naruta, Y.; Yamauchi, O. *J. Am. Chem. Soc.* **2003**, *125*, 10512. (b) Shimazaki, Y.; Yajima, T.; Tani, F.; Karasawa, S.; Fukui, K.; Naruta, Y.; Yamauchi, O. *J. Am. Chem. Soc.* **2007**, *129*, 2559. (c) Shimazaki, Y.; Arai, N.; Dunn, T. J.; Yajima, T.; Tani, F.; Ramogida, C. F.; Storr, T. *Dalton Trans.* **2011**, *40*, 2469.
(39) Dunn, T. J.; Ramogida, C. F.; Simmonds, C.; Paterson, A.; Wong, E. W. Y.; Chiang, L.; Shimazaki, Y.; Storr, T. *Inorg. Chem.* **2011**, *50*, 6746.
(40) Kochem, A.; Jarjayes, O.; Baptiste, B.; Philouze, C.; Vezin, H.; Tsukidate, K.; Tani, F.; Orio, M.; Shimazaki, Y.; Thomas, F. *Chem.—Eur. J.* **2012**, *18*, 1068.
(41) For example, see: (a) Amimoto, K.; Kawato, T. *J. Photochem. Photobiol., C* **2005**, *6*, 207. (b) Sekikawa, T.; Kobayashi, T. *J. Phys. Chem. B* **1997**, *101*, 10645. (c) Oshima, A.; Momotake, A.; Arai, T. *Chem. Lett.* **2005**, *34*, 1288. (d) Fita, P.; Luzina, E.; Dziembowska, T.; Radzewicz, Cz.; Grabowska, A. *J. Chem. Phys.* **2006**, *125*, 184508.
(42) The dielectric constant ε_{mix} of the binary mixture of solvents A and B with dielectric constants ε_A and ε_B was estimated according to the following equation: $(\varepsilon_{mix} - 1)/(\varepsilon_{mix} + 2) = ((\varepsilon_A - 1)/(\varepsilon_A + 2))x_A + ((\varepsilon_B - 1)/(\varepsilon_B + 2))x_B$, where x_A and x_B are the volume fractions of A and B.
(43) The procedure for the arithmetic treatment was as follows: (Step 1) A series of spectral data were stored as $f_1, f_2, f_3, ..., f_9$, in increasing order of solvent polarity. (Step 2) $\Delta f_{2-1} = f_2 - f_1$ was calculated and stored as an increment of the $\mathbf{1}_{NH/OH}$ contribution (f_1, f_5, and f_9 are the spectra measured for pure MCH, THF, and EtOH solution, respectively). (Step 3) $f_{OH/OH} = f_1 - 0.0883\Delta f_{2-1}$ was calculated so that the $\mathbf{1}_{NH/OH}$ contribution could be virtually removed from f_1. (Step 4) $\Delta f_{5-4} = f_5 - f_4$ was calculated and stored as a decrement of the $\mathbf{1}_{OH/OH}$ contribution. (Step 5) $f_{NH/OH} = f_5 - 13.0\Delta f_{5-4}$ was calculated so that the $\mathbf{1}_{OH/OH}$ contribution could be virtually removed from f_5. (Step 6) $f_{NH/NH} = f_9 - 0.807 f_{NH/OH}$ was calculated so that the $\mathbf{1}_{NH/OH}$ contribution could be virtually removed from f_9.
(44) Hara, S.; Houjou, H.; Yoshikawa, I.; Araki, K. *Cryst. Growth Des.* **2011**, *11*, 5113.
(45) Pope, M.; Swenberg, C. *Electronic Process in Organic Crystals and Polymers*, 2nd ed.; Oxford University Press: New York, 1999.
(46) Kruszewski, J.; Krygowski, T. M. *Tetrahedron Lett.* **1972**, *36*, 3839.
(47) Krygowski, T. M.; Palusiak, M.; Plonka, A.; Zachara-Horeglad, J. E. *J. Phys. Org. Chem.* **2007**, *20*, 297.
(48) Filarowski, A.; Kochel, A.; Kluba, M.; Komounah, F. S. *J. Phys. Org.Chem.* **2008**, *21*, 939.
(49) Grabowski, S. J. *J. Phys. Org. Chem.* **2003**, *16*, 797.
(50) Palusiak, M.; Simon, S.; Solà, M. *J. Org. Chem.* **2006**, *71*, 5241.
(51) Palusiak, M.; Krygowski, T. M. *Chem.—Eur. J.* **2007**, *13*, 7996.
(52) Krygowski, T. M.; Zachara, J. E.; Ośmiałowski, B.; Gawinecki, R. *J. Org. Chem.* **2006**, *71*, 7678.
(53) Mohajeri, A. *J. Mol. Struct.: THEOCHEM* **2004**, *678*, 201.
(54) Zborowski, K.; Proniewicz, L. M. *J. Phys. Org. Chem.* **2008**, *21*, 207.
(55) Jezierska-Mazzarello, A.; Szatyłowicz, H.; Krygowski, T. M. *J. Mol. Model.* **2012**, *18*, 127.
(56) Grabowski, S. J. *J. Phys. Org. Chem.* **2003**, *16*, 797.
(57) Sheldrick, G. M. *Acta Crystallogr.* **2008**, *A64*, 112.
(58) Frisch, M. J.; Trucks, G. W.; Schlegel, H. B.; Scuseria, G. E.; Robb, M. A.; Cheeseman, J. R.; Montgomery, J. A., Jr.; Vreven, T.; Kudin, K. N.; Burant, J. C.; Millam, J. M.; Iyengar, S. S.; Tomasi, J.; Barone, V.; Mennucci, B.; Cossi, M.; Scalmani, G.; Rega, N.; Petersson, G. A.; Nakatsuji, H.; Hada, M.; Ehara, M.; Toyota, K.; Fukuda, R.; Hasegawa, J.; Ishida, M.; Nakajima, T.; Honda, Y.; Kitao, O.; Nakai, H.; Klene, M.; Li, X.; Knox, J. E.; Hratchian, H. P.; Cross, J. B.; Adamo, C.; Jaramillo, J.; Gomperts, R.; Stratmann, R. E.; Yazyev, O.; Austin, A. J.; Cammi, R.; Pomelli, C.; Ochterski, J. W.; Ayala, P. Y.; Morokuma, K.; Voth, G. A.; Salvador, P.; Dannenberg, J. J.; Zakrzewski, V. G.; Dapprich, S.; Daniels, A. D.; Strain, M. C.; Farkas, O.; Malick, D. K.; Rabuck, A. D.; Raghavachari, K.; Foresman, J. B.; Ortiz, J. V.; Cui, Q.; Baboul, A. G.; Clifford, S.; Cioslowski, J.; Stefanov, B. B.; Liu, G.; Liashenko, A.; Piskorz, P.; Komaromi, I.; Martin, R. L.; Fox, D. J.; Keith, T.; Al-Laham, M. A.; Peng, C. Y.; Nanayakkara, A.; Challacombe, M.; Gill, P. M. W.; Johnson, B.; Chen, W.; Wong, M. W.; Gonzalez, C.; Pople, J. A. *Gaussian 03*, revision C.02; Gaussian, Inc.: Wallingford, CT, 2004.
(59) Frisch, M. J.; Trucks, G. W.; Schlegel, H. B.; Scuseria, G. E.; Robb, M. A.; Cheeseman, J. R.; Scalmani, G.; Barone, V.; Mennucci, B.; Petersson, G. A.; Nakatsuji, H.; Caricato, M.; Li, X.; Hratchian, H. P.; Izmaylov, A. F.; Bloino, J.; Zheng, G.; Sonnenberg, J. L.; Hada, M.; Ehara, M.; Toyota, K.; Fukuda, R.; Hasegawa, J.; Ishida, M.; Nakajima, T.; Honda, Y.; Kitao, O.; Nakai, H.; Vreven, T.; Montgomery, J. A., Jr.; Peralta, J. E.; Ogliaro, F.; Bearpark, M.; Heyd, J. J.; Brothers, E.; Kudin, K. N.; Staroverov, V. N.; Kobayashi, R.; Normand, J.; Raghavachari, K.; Rendell, A.; Burant, J. C.; Iyengar, S. S.; Tomasi, J.; Cossi, M.; Rega, N.; Millam, J. M.; Klene, M.; Knox, J. E.; Cross, J. B.; Bakken, V.; Adamo, C.; Jaramillo, J.; Gomperts, R.; Stratmann, R. E.; Yazyev, O.; Austin, A. J.; Cammi, R.; Pomelli, C.; Ochterski, J. W.; Martin, R. L.; Morokuma, K.; Zakrzewski, V. G.; Voth, G. A.; Salvador, P.; Dannenberg, J. J.; Dapprich, S.; Daniels, A. D.; Farkas, O.; Foresman, J. B.; Ortiz, J. V.; Cioslowski, J.; Fox, D. J. *Gaussian 09*, revision A.02; Gaussian, Inc.: Wallingford, CT, 2009.